# Effect of Shear History on Flow Instability at Capillary Extrusion for Long-Chain Branched Polyethylene

**Siriprumpoonthum Monchai, Naoya Mieda, Vu Anh Doan, Shogo Nobukawa, Masayuki Yamaguchi**

*School of Materials Science, Japan Advanced Institute of Science and Technology, 1-1 Asahidai, Nomi, Ishikawa 923-1292, Japan*

Received 26 April 2011; accepted 17 June 2011
DOI 10.1002/app.35108
Published online 4 October 2011 in Wiley Online Library (wileyonlinelibrary.com).

**ABSTRACT:** Effect of applied processing history on flow instability at capillary extrusion is studied using a commercially available low-density polyethylene (LDPE) having long-chain branches. It is found that processing history in an internal mixer in a molten state depresses long-time relaxation mechanism associated with long-chain branches, which is known as "shear modification." Consequently, the onset of output rate for melt fracture increases greatly. Furthermore, it should be noted that the sample having intense shear history shows shark-skin failure without volumetric distortion, although it has been believed that LDPE exhibits gross melt fracture at capillary extrusion. The reduction of elongational viscosity by the alignment of long-chain branches along to the main chain is responsible for the anomalous rheological response. As a result, the sample shows shark-skin failure like a linear polyethylene at a lower output rate than the critical one for gross melt fracture. © 2011 Wiley Periodicals, Inc. J Appl Polym Sci 124: 429–435, 2012

**Key words:** polymer extrusion; rheology; polyethylene; melt; viscoelastic properties

## INTRODUCTION

It is well known that long-chain branches enhance the elastic features greatly in a molten state.[1–8] Therefore, a low-density polyethylene (LDPE) produced by a radical polymerization method under high pressure, which is characterized as a long-chain branched polymer, shows higher melt elasticity than a conventional linear LLDPE obtained by copolymerization of ethylene and α-olefin with the aid of Zieglar–Natta or metallocene catalyst. However, the elastic property of LDPE in a molten state is found to be depressed by applied processing history, which is known as "shear modification."[9–19]

The mechanism of the shear modification was explained by Münstedt[13] based on the tube model proposed by Doi and Edward.[4] According to the tube model, a branch polymer shows prolonged characteristic time of the longest relaxation mechanism at the equilibrium state, because a simple reptation is not allowed by the branch parts. Furthermore, the chain contraction between branch points is prohibited, which is responsible for the marked strain-hardening behavior in transient elongational viscosity. After processing history, long-chain branches tend to align to the main chain by applied hydrodynamic force.[7,13,15] Consequently, a branch part is dragged into a tube of a main chain, leading to decrease in "active" long-chain branches. Therefore, the polymer behaves like a linear polymer having low melt elasticity. The alignment of branch parts, however, will be relaxed after cessation of flow because of the low entropy state around the branch points. Yamaguchi and Gogos evaluated the rheological properties at recovery process from "shear modification" and found that the rheological properties after applied shear history are determined by the shear stress and the duration time of shearing.[17] This is reasonable, because degree of molecular orientation increases with the stress, known as the stress-optical law.

The marked strain-hardening behavior in transient elongational viscosity for LDPE is responsible for good processability at various processing operations such as reduction of draw resonance and small level of neck-in at T-die extrusion, uniform wall thickness, and reduction of heat sagging at blow-molding and thermoforming, and large expansion ratio with fine cell structure at foaming.[20–28] However, gross volumetric melt fracture occurs for LDPE even at low-output rate condition, which limits productivity at extrusion. On the contrary, shark-skin failure, that is, minute surface roughness of extrudates, decides the productivity for linear polyethylenes such as LLDPE and high-density polyethylene (HDPE). In other words, the type of flow instability at capillary

*Correspondence to:* M. Yamaguchi (m_yama@jaist.ac.jp).

extrusion for polyethylene is dependent upon the molecular structure.

The mechanism of flow instability at capillary extrusion has been studied for a long time.[29–45] The gross melt fracture is the flow instability occurred at die entrance, which is prominent for a polymer melt with high melt elasticity, such as LDPE and poly(vinyl chloride).[45,46] Meller found that elongational stress generated by contraction flow at die entrance decides the occurrence of gross melt fracture.[36] As increasing the output rate, gross melt fracture occurs when the elongational stress is beyond the critical one. Since LDPE exhibit marked strain-hardening in elongational viscosity, leading to high elongational stress, gross melt fracture is always detected. Recently, Mieda and Yamaguchi revealed that binary blends of LDPE and LLDPE with high molecular weight exhibit severe gross melt fracture owing to enhanced elongational stress.[45] On the contrary, LLDPE and HDPE show shark-skin failure before gross melt fracture when shear stress is beyond the critical value. Roughly speaking, two types of mechanism have been proposed for shark-skin failure; one is owing to cohesive rupture at surface of extrudates by sudden large deformation at die exit, originally proposed by Cogswell[30]; and the other is due to the detachment of a melt from die surface accompanied with cracks by adhesive failure, which was summarized in recent works by Kulikov et al.[39,43] Moreover, the critical stresses of shark-skin failure of both mechanisms were theoretically derived by Allal et al.,[42] which agree with the experimental data obtained by Yamaguchi et al.[37] using model polyolefins. Yamaguchi et al.[37,44,45] also explained the onset of shark-skin failure as well as gross melt fracture using the concept of Deborah number. Although their explanation does not predict the mechanism, it provides the direction to solve the problem.

The difference in the type of flow instability between LDPE and linear polyethylenes suggests that LDPE reaches to the critical elongational stress of gross melt fracture before the critical shear stress of shark-skin failure and vice versa.[36] Consequently, LDPE, showing high level of elongational stress, always exhibits gross melt fracture at first without shark-skin failure in general. In fact, shark-skin failure of LDPE without volumetric distortion has not been reported yet to the best of our knowledge.

In this study, the effect of processing history on the flow instability at capillary extrusion is evaluated using LDPE. Because processing history weakens the strain-hardening behavior in elongational viscosity for LDPE, the type of flow instability at capillary extrusion can be changed. This will be important information on extrusion processing of LDPE, because the flow instability decides the output rate at actual processing, that is, productivity.

## EXPERIMENTAL

### Materials

The LDPE [melt flow rate = 1.6 (g/10 min) at 190°C under 2.16 kg] used in this study was a commercial material produced by a radical polymerization method in an autoclave reactor (Tosoh, Petrocene 360).

The number–, weight–, and *z*–average molecular weights were measured by gel permeation chromatography (Waters, 150°C) at 135°C, in which *ortho*-dichlorobenzene was used as a solvent. The flow rate was 1.0 mL/min, and the sample concentration was 1.0 mg/mL. It is found that $M_n = 2.6 \times 10^4$, $M_w = 2.1 \times 10^5$, and $M_z = 6.7 \times 10^5$, respectively.

The species and contents of branches estimated by $^{13}$C-nuclear magnetic resonance spectroscopy are as follows: 7 butyl, 2 pentil, and 5 hexyl and longer branches per 1000 backbone carbon atoms.

Further information on molecular characteristics such as shrinking factor as well as various viscoelastic properties has been reported in our previous works.[16–18,46–49]

### Sample preparation

Processing histories were applied to LDPE in a laboratory-scale counter-rotating internal mixer with blade-type rotors at 160°C (Toyoseiki, Labo-plastmil) for various residence times at 30 rpm of the blade rotation speed. The amount of the sample in the mixer was 48 g, that is, fullfilling condition. Furthermore, thermal stabilizers such as pentaerythritol tetrakis (3-3,5-di-*tert*-butyl-4-hydroxyphenyl) propionate (Ciba, Irganox1010) and tris(2,4-di-*tert*-butylphenyl)phosphate (Ciba, Irgafos168) were added to prohibit thermal degradation, with calcium stearate as a neutralizer. The amount of each additive was 5000 ppm. The residence time in the mixer was decided considering the thermal stability as well as the homogeneity in the sample from the viewpoints of kneading, that is, processing history.

Furthermore, the obtained samples were compressed into a flat sheet by a compression-molding machine (Tester Sangyo, SA303IS) at 160°C under 10 MPa for 3 min. Then, the sample was subsequently cooled down. After cutting the samples, various rheological properties were evaluated.

### Measurements

The frequency dependence of oscillatory shear moduli was measured by a cone-and-plate rheometer (TA Instruments, AR-2000ex) at 160, 190, and 230°C under nitrogen atmosphere. The cone angle was 5°, and the diameter was 25 mm. When measuring the processed sample, time dependence of shear moduli

at various frequencies was evaluated at 160°C, because the moduli grow rapidly with time by the thermal history in the rheometer. The detail in the measurement method for the processed sample was mentioned in the references.[17,46]

The drawdown force, defined as the force required for the extension of a polymer melt at a constant stretching ratio, was evaluated at 160°C by a capillary rheometer (Yasuda Seiki Seisakusyo, 140 SAS-2002) equipped with a tension detector (Nidec-Shimpo, tensionmeter PLS) and a set of rotating wheels. The dimension of the capillary die was as follows: 8 mm in length $L$, 2.095 mm in diameter $D$, and an entrance angle of $\pi/2$. The drawdown force was evaluated at a draw ratio of 7. Considering that the drawdown force increases with the residence time in the capillary rheometer as demonstrated by Yamaguchi et al.,[16,17,50] the measurement was performed with a constant residence time, 3 min, in the barrel of the capillary rheometer.

The apparent shear viscosity was also measured by the capillary rheometer using another circular die having $L/D = 10/1$ (mm) at 160°C. Furthermore, the appearance of the extruded strands was examined by an optical microscope (Leica, S6E) and a scanning electron microscope (SEM; Hitachi, S400). Before SEM observation, the samples were coated by Pt-Pd.

The transient uniaxial elongational viscosity was measured by a Meissner-type rheometer (Toyoseiki, Melten Rheometer) in an oil bath at various elongational strain rates at 160°C. Rod samples were prepared by the capillary rheometer.

## RESULTS AND DISCUSSION

### Linear viscoelastic properties of original LDPE

Figure 1 shows the master curves of frequency dependence of oscillatory shear modulus at 160°C for LDPE without the processing history in the internal mixer. As a comparison, the shear moduli for the sample processed in the mixer for 120 min are also plotted. The viscoelastic properties of the virgin LDPE, which suggest broad distribution of relaxation time, are typical ones for a commercially available LDPE. The oscillatory modulus is, however, known to be insensitive to the difference in branch structure for polyethylenes.[27,51] In particular, it is almost impossible to predict the processability such as the level of neck-in by oscillatory shear modulus.

The flow activation energy is calculated to discuss the branch structure assuming that the time-temperature superposition principle is applicable to the virgin LDPE and found to be $\sim$ 53 kJ/mol. The value, however, has no/little relation with, at least, long-chain branch structure for a commercial LDPE,[16] although it is known that longer branches

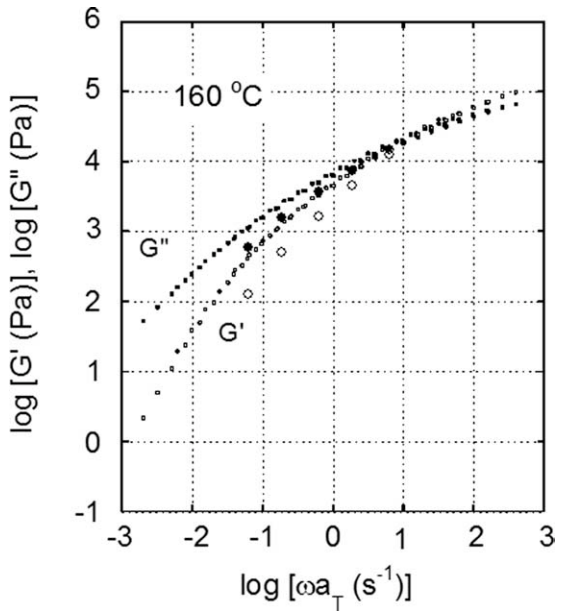


**Figure 1** Master curves of frequency dependence of oscillatory shear moduli such as (open symbols) storage modulus $G'$ and (closed symbols) loss modulus $G''$ at 160°C for (small symbols) virgin LDPE and (large symbols) LDPE processed by the mixer for 120 min. The figure is reproduced from a part of the data in Ref. 16.

provide higher activation energy employing model star-branch polyethylenes.[52,53] This could be attributed to the complicated branch structure for a commercial LDPE. Moreover, some LDPE samples are known to be thermocomplex materials,[45,46,49] although Stadler et al.[54] reported that LDPE used in their research obeys the time-temperature superposition principle. This is reasonable because relaxation mechanism associated with long-chain branches has different activation energy from that of entanglement couplings for a linear polyethylene.[5,52,53] We confirmed that the present LDPE is also a thermocomplex material as demonstrated by a well-known van Gurp–Palmen plot in our previous work.[49]

In case of the processed sample, a conventional frequency sweep method is not appropriate to measure the oscillatory moduli, because the values grow by the thermal history in the rheometer, as demonstrated in detail by Yamaguchi and Gogos.[17] Therefore, time dependence of oscillatory moduli was measured at various frequencies. Then, the value at $t = 0$, that is, oscillatory moduli for processed LDPE without postprocessing annealing was estimated at each frequency. Furthermore, the measurements were performed only at 160°C because of the same reason. As seen from the figure, both moduli drop to a great extent by the processing history in the internal mixer with an intense fashion of $G'$, which is the same results in our previous work.[17]

### Rheological properties under elongational flow

Figure 2 shows the drawdown force as a function of the residence time in the internal mixer. It is found that the drawdown force of virgin pellets having no processing history in the internal mixer is significantly high, 580 ± 30 mN. However, the value drops off sharply with the processing history. For example, the drawdown force of the sample processed for 120 min is only 100 ± 10 mN, which is lower than 20% of the original value. Furthermore, the value is almost similar to that of LLDPE having a similar shear viscosity.[55] The sample shows neither molecular scission nor crosslinking reaction at the present processing condition, which is confirmed by gel permeation chromatography as shown in Figure 3. Therefore, the sensitivity of drawdown force to the applied processing history would be attributed to the reduction of strain-hardening behavior. This is the phenomenon of the shear modification. Consequently, the drawdown force recovers to the initial high value after annealing treatment beyond the melting point without flow field.[16,17]

Figure 4 shows the growth curves of uniaxial elongational viscosity at various strain rates for the virgin LDPE and LDPE processed for 15 min in the internal mixer. The solid line in the figure represents the growth curve in the linear region calculated from the oscillatory shear moduli, that is, three time of transient shear viscosity at low-strain rate asymptote $3\eta^+(t)$. As seen from the figure, marked strain-hardening behavior is detected for the virgin LDPE, which is reduced to a great extent by the exposure to processing history. On the contrary, the magnitude in the linear region of the elongational viscosity is not changed to a great extent. Furthermore, the measurement cannot be performed for the samples processed for 30 and 120 min because of severe sagging by gravitational force.

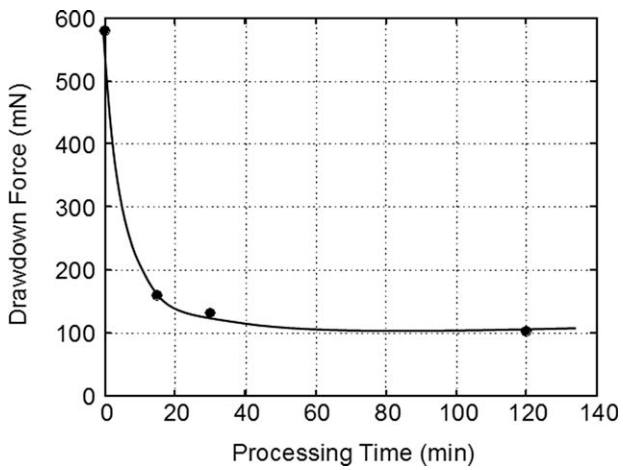


**Figure 2** Drawdown force of LDPE as a function of the processing time in the internal mixer at 160°C. The extrapolated line is inserted to see the result clearly.

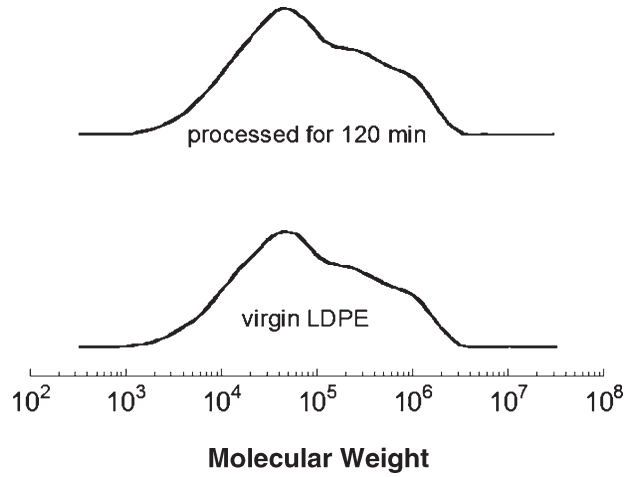


**Figure 3** GPC curves of virgin LDPE and LDPE processed for 120 min in the mixer.

Strain-hardening index, defined as the ratio of the highest elongational viscosity to the linear value at the same time, is evaluated from the data at the intermediate strain rate to minimize the experimental error and found to be 10.2 for the virgin LDPE and 4.3 for the sample processed for 15 min.

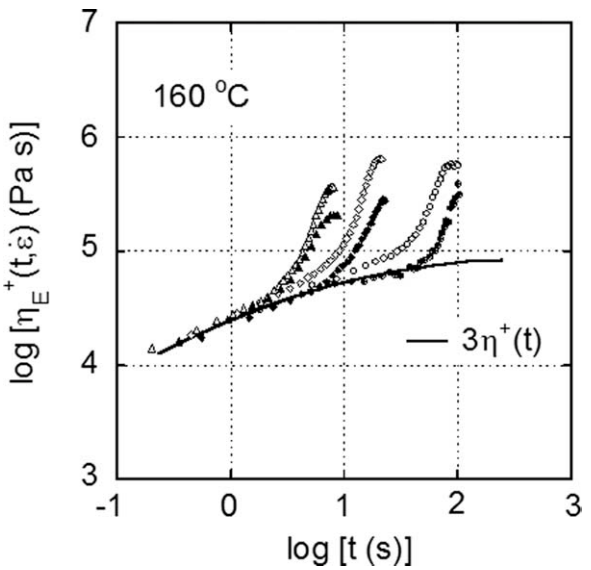


**Figure 4** Growth curves of uniaxial elongational viscosity at various strain rates at 160°C for (open symbols) virgin LDPE and (closed symbols) LDPE processed by the internal mixer for 15 min. The solid line represents three time of transient shear viscosity calculated from the oscillatory shear moduli. The applied elongational strain rates are (open circles) 0.038 $s^{-1}$, (open diamonds) 0.16 $s^{-1}$, (open triangles) 0.36 $s^{-1}$, (closed circles) 0.041 $s^{-1}$, (closed diamonds) 0.18 $s^{-1}$, and (closed triangles) 0.37 $s^{-1}$. The data of the virgin LDPE are reproduced from a part of the data in Ref. 16.

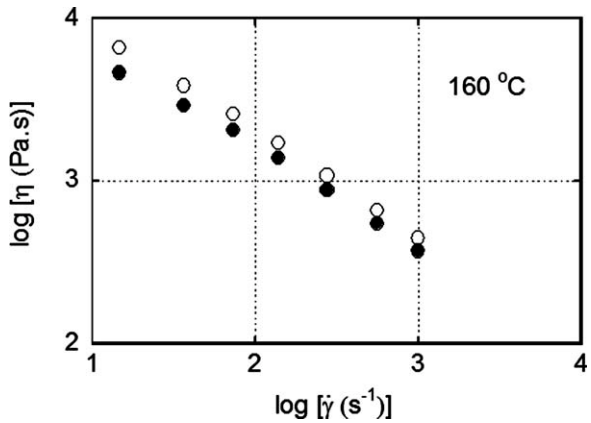


**Figure 5** Flow curves at 160°C for (open symbols) LDPE and (closed symbols) LDPE processed for 120 min.

### Capillary extrusion

The flow curves at 160°C without Rabinowitch and Bagley corrections are shown in Figure 5. The values, whose experimental errors are minuscule, are slightly higher than those calculated from oscillatory moduli by Cox–Merz relation. A part of the origin of the deviation could be attributed to the difference in end-pressure drop at the capillary exit.

As seen from the figure, the sample shows non-Newtonian behavior in the experimental shear rate region irrespective of the processing history. Because relaxation mechanism with long characteristic time is weakened by shear modification,[17] shear viscosity of the sample after the processing history is slightly lower than that of the virgin LDPE, which is pronounced in the low-shear rate region.

Figure 6 shows the apparent wall shear stress with pictures of the extruded strands. Both samples exhibit smooth surface without any distortion at low shear stress. As increasing the shear rate and thus the output rate, the virgin LDPE exhibits volumetric distortion with smooth surface at 73 $s^{-1}$ ($1.9 \times 10^5$ Pa) and 140 $s^{-1}$ ($2.4 \times 10^5$ Pa). Beyond 280 $s^{-1}$, surface of the distorted strand becomes rough. The magnified pictures observed by SEM are shown in Figure 7.

On the contrary, the processed sample can be extruded without melt fracture at 140 $s^{-1}$ ($1.9 \times 10^5$

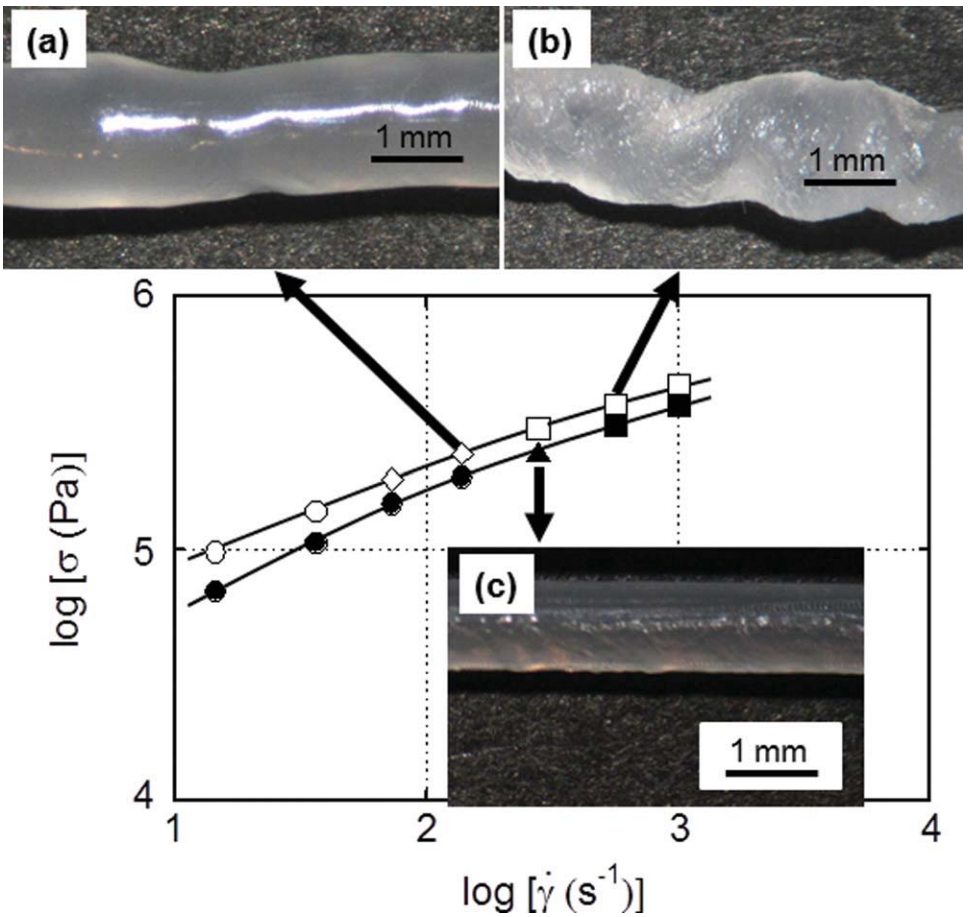


**Figure 6** Shear stress as a function of shear rate at 160°C with pictures of extrudates for (open symbols) LDPE and (closed symbols) LDPE processed for 120 min; (circles) smooth surface without gross melt fracture, (triangles) shark-skin failure without gross melt fracture, (diamonds) gross melt fracture with smooth surface, and (squares) gross melt fracture with rough surface. [Color figure can be viewed in the online issue, which is available at wileyonlinelibrary.com.]

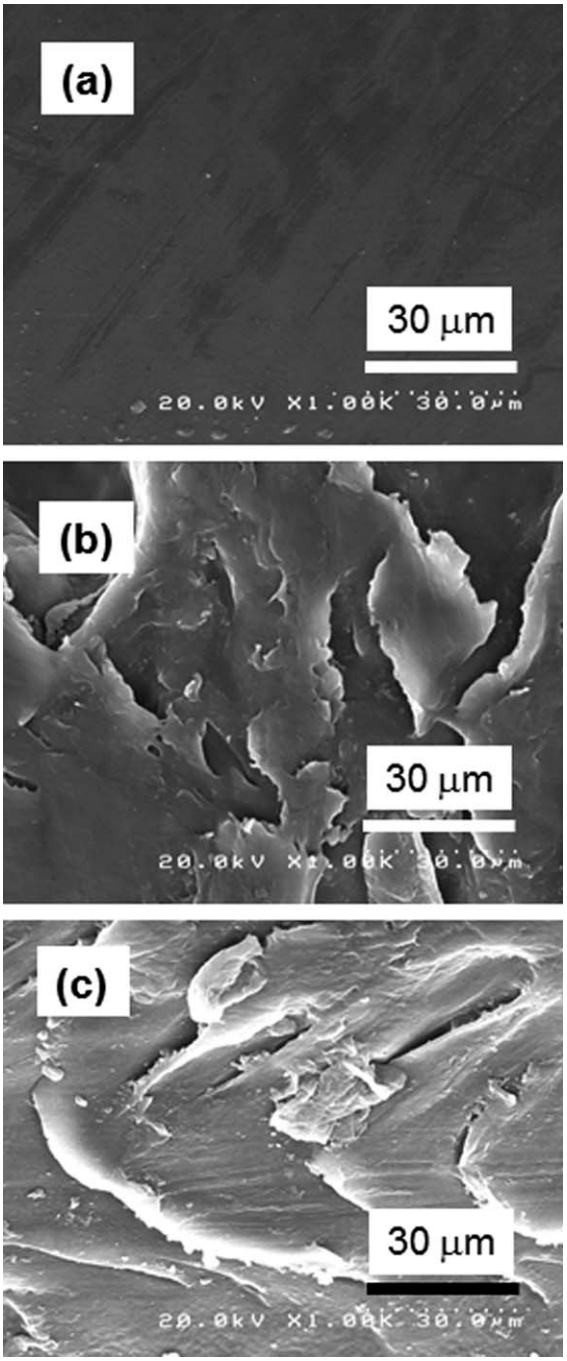


**Figure 7** SEM pictures of the extrudates' surface; (a) 140 $s^{-1}$ for virgin LDPE, (b) 560 $s^{-1}$ for virgin LDPE, and (c) 280 $s^{-1}$ for LDPE processed for 120 min.

Pa), even though the shear stress is slightly higher than that at 73 $s^{-1}$ for the virgin LDPE. This is a great benefit for actual extrusion processing, because it can be operated at high-output rate condition. Considering that the gross melt fracture appears beyond the critical elongational stress, the processed sample shows lower elongational stress owing to the reduced strain-hardening behavior in elongational viscosity as shown in Figure 3. Furthermore, the great depression of the drawdown force with small reduction of shear viscosity also indicates weak strain-hardening.

Moreover, shark-skin failure is detected at 280 $s^{-1}$ ($2.4 \times 10^5$ Pa) without volumetric distortion for the processed sample, although it has been believed that LDPE shows gross melt fracture at first not shark-skin failure. As seen from Figure 7(c), it seems that the crack of adhesive failure at the die wall propagates to large scale roughness, which is a similar result reported by Kulikov et al.[39,43] Beyond 560 $s^{-1}$, the processed sample also shows gross melt fracture with rough surface.

Finally, it can be concluded that rheological properties of processed LDPE are similar to those of LLDPE and HDPE from a viewpoint of flow instability. The applied processing history, leading to low elongational stress, avoids the onset of the gross melt fracture.

## CONCLUSIONS

The effect of processing history on the flow instability at capillary extrusion is studied using LDPE. It is found that the shark-skin failure occurs for LDPE at capillary extrusion after exposure to shear history for a long time. Because the applied flow history depresses the strain-hardening behavior in elongational viscosity owing to shear modification, the elongational stress at die entry at extrusion will be reduced to a great extent. As a result, the stress level becomes lower than the critical elongational stress of gross melt fracture. As increasing the output rate, shark-skin failure appears when the applied shear stress at die exit is beyond the critical shear stress of shark-skin failure. This experimental result demonstrates that LDPE behaves as a linear polyethylene from the view point of flow instability. As a result, the processed LDPE is available for extrusion processing at high-output rate condition, because the onset value of flow instability increases greatly.

## References

1. Boghetich, L.; Kratz, R. F. Trans Soc Rheol 1965, 9, 255.
2. Mendelson, R. A.; Bowles, W. A.; Finger, F. L. J Polym Sci Polym Phys Ed 1970, 8, 105.
3. Ferry, J. D. Viscoelastic Properties of Polymers; Wiley: New York, 1980.
4. Doi, M.; Edwards, S. F. The Theory of Polymer Dynamics; Clarendon Press: Oxford, 1986.
5. Vega, J. F.; Santamaria, A. Macromolecules 1998, 31, 3639.
6. Gotsis, A. D.; Zeevenhoven, B. L. F.; Tsenoglou, C. J Rheol 2004, 48, 895.
7. Yamaguchi, M. In Polymeric Foam, Mechanisms and Materials; Lee, S. T., Ramesh, N. S., Eds.; CRC Press: New York, 2004; Chapter 2.
8. Münstedt, H. Soft Matter 2011, 7, 227.
9. Howells, E. R.; Benbow, J. J Trans J Plast Inst 1962, 30, 240.
10. Hanson, D. E. Polym Eng Sci 1969, 9, 405.

11. Fujiki, T. J Appl Polym Sci 1969, 13, 233.
12. Rokudai, M. J Appl Polym Sci 1979, 23, 463.
13. Münstedt, H. Colloid Polym Sci 1981, 259, 966.
14. Rudin, A.; Schreiber, H. P. Polym Eng Sci 1983, 23, 422.
15. Leblans, P. J. R.; Bastiaansen, C. Macromolecules 1989, 22, 3312.
16. Yamaguchi, M.; Takahashi, M. Polymer 2001, 42, 8663.
17. Yamaguchi, M.; Gogos, C. G. Adv Polym Technol 2001, 20, 261.
18. Yamaguchi, M.; Todd, D. B.; Gogos, C. G. Adv Polym Technol 2003, 22, 179.
19. Marin, G.; Bourrigaud, S.; Poitou, A. Macromolecules 2003, 36, 1388.
20. Debroth, T.; Erwin, L. Polym Eng Sci 1986, 26, 462.
21. Phillips, E. M.; McHugh, K. E.; Bradley, M. B. J Coat Fabrics 1990, 19, 155.
22. Park, C. B.; Cheung, L. K. Polym Eng Sci 1997, 37, 1.
23. Lau, H. C.; Bhattacharya, S. N.; Field, G. J Polym Eng Sci 1998, 38, 1915.
24. Field, G. J.; Micic, P.; Bhattacharya, S. N. Polym Int 1999, 48, 461.
25. Yamaguchi, M.; Suzuki, K. J Polym Sci Polym Phys Ed 2001, 39, 2159.
26. Yamaguchi, M.; Suzuki, K. J Appl Polym Sci 2002, 86, 79.
27. Kouda, S. Polym Eng Sci 2008, 48, 1094.
28. Ono, K.; Ogita, H.; Okamoto, K.; Yamaguchi, M. J Appl Polym Sci 2009, 113, 3368.
29. Tordera, J. J Appl Phys 1963, 7, 215.
30. Cogswell, F. N. Polymer Melt Rheology; George Godwin Ltd: London, 1981.
31. Ramamurthy, A. V. J Rheol 1986, 30, 337.
32. Brochard, F.; de Gennes, P. G. Langmuir 1992, 8, 3033.
33. Piau, J. M.; Agassant, J. F. Rheology for Polymer Melt Processing; Elsevier: Amsterdam, 1996.
34. Denn, M. M. Annu Rev Fluid Mech 2001, 33, 265.
35. Fujiyama, M. J Appl Polym Sci 2002, 84, 2120.
36. Meller, M.; Luciani, A.; Sarioglu, A.; Manson, J. E. Polym Eng Sci 2002, 42, 611.
37. Yamaguchi, M.; Miyata, H.; Tan, V.; Gogos, C. G. Polymer 2002, 43, 5249.
38. Hatzikiriakos, S. G.; Migler, K. B. Polymer Processing Instabilities; Marcel Dekker: New York, 2005.
39. Kulikov, O. J Vinyl Additive Technol 2005, 11, 127.
40. Tadmor, Z.; Gogos, C. G. Principles of Polymer Processing, 2nd ed.; Willy-Interscience: New York, 2006.
41. Wang, X.; Wang, X. Y.; Wang, Z.; Hee, J. J Macromol Sci B Phys 2006, 45, 777.
42. Allal, A.; Vergnes, B. J Non-Newtonian Fluid Mech 2007, 146, 45.
43. Kulikov, O.; Hornung, K.; Wagner, H. M. Rheol Acta 2007, 46, 741.
44. Suzuki, M.; Amran, M. A. M.; Okamoto, K.; Taniike, T.; Terano, M.; Yamaguchi, M. Adv Polym Technol 2009, 28, 185.
45. Mieda, N.; Yamaguchi, M. J Non-Newtonian Fluid Mech 2011, 166, 231.
46. Yamaguchi, M. J Appl Polym Sci 2001, 82, 1277.
47. Yamaguchi, M. J Appl Polym Sci 2006, 102, 1078.
48. Wagner, M. H.; Yamaguchi, M.; Takahashi, M. J Rheol 2003, 47, 779.
49. Wagner, M. H.; Kheirandish, S.; Yamaguchi, M. Rheol Acta 2004, 44, 198.
50. Yamaguchi, M.; Wagner, M. H. Polymer 2006, 47, 3629.
51. Ono, K.; Yamaguchi, M. J Appl Polym Sci 2009, 113, 1462.
52. Lohse, D. J.; Milner, S. T.; Fetters, L. J.; Xenidon, M.; Hadjichristids, N.; Mendelson, R. A.; Garcia-France, C. A.; Lyon, M. K. Macromolecules 2002, 35, 3066.
53. Graessley, W. W.; Raju, V. R. J Polym Sci Polym Symp 1984, 71, 77.
54. Stadler, F. J.; Kaschta, J.; Münstedt, H. Macromolecules 2008, 41, 1328.
55. Mieda, N.; Yamaguchi, M. Adv Polym Technol 2007, 26, 173.